2011

Eliminating Electromechanic Instablity in Dielectric Elastomers by Employing Pre-stretch

Liang Jiang
Technological University Dublin

Tony Betts
Technological University Dublin, anthony.betts@tudublin.ie

David Kennedy
Technological University Dublin, david.kennedy@tudublin.ie

Stephen Jerrams
Technological University Dublin, stephen.jerrams@tudiblin.ie

Recommended Citation

Jiang, L., Betts, A., Kennedy, D. & Jerrams, S. (2011). Eliminating electromechanical instability in dielectric elastomers by employing pre-stretch. *Journal of Physics D: Applied Physics*, vol. 44, no. 15, pg. 155301. doi:10.1088/0022-3727/44/15/155301

Eliminating electromechanical instability in dielectric elastomers by employing pre-stretch

Liang Jiang [1, a], Anthony Betts [b], David Kennedy [c], Stephen Jerrams [a]

[a] Centre for Elastomer Research, Focas Research Institute, Dublin Institute of Technology, Dublin 8, Ireland

[b] Applied Electrochemistry Group, Focas Research Institute, Dublin Institute of Technology, Dublin 8, Ireland

[c] Department of Mechanical Engineering, Dublin Institute of Technology, Dublin 1, Ireland

Abstract

Electromechanical instability (EMI) is one of most common failure modes for dielectric elastomers (DEs). It has been reported that pre-stretching a DE sample can suppress EMI due to strain stiffening taking place for larger strains and a higher elastic modulus are achieved at high stretch ratios when a voltage is applied to the material. In this work, the influence of equi-biaxial stretch on DE secant modulus was studied using VHB 4910 and silicone rubber (SR) composites containing barium titanate ($BaTiO_3$, BT) particles and also dopamine coated BT (DP-BT) particles. The investigation of equi-biaxial deformation and EMI failure for VHB 4910 was undertaken by introducing a voltage-stretch function. The results showed that EMI was suppressed by equi-biaxial pre-stretch for all the DEs fabricated and tested. The stiffening properties of the DE materials were also studied with respect to the secant modulus. Furthermore, a voltage-induced strain of above 200% was achieved for the polyacrylate film by applying a pre-stretch ratio of 2.0 without EMI occurring. However, a maximum voltage-induced strain in the polyacrylate film of 78% was obtained by the SR/20 wt% DP-BT composite for a lower applied pre-stretch ratio of 1.6 and again EMI was eliminated.

Keywords: Dielectric elastomers; Mechanical model; Equi-biaxial mechanical test; Electromechanical instability

1. Introduction

DEs belong to the family of smart materials and can exhibit large deformations when high voltages are applied to them. Owing to large voltage-induced strain, high electromechanical coupling efficiency, light weight, inherent compliance, low cost and absence of noise pollution, DEs are proposed for many applications such as haptic displays [1], acoustic transducers [2], pneumatic valves [3] and power generators [4, 5]. Generally, a DE has compliant electrodes sprayed onto its top and bottom surfaces and usually a pre-stretch is applied (Fig. 1(a)). When subjected to a large electric field, an electrostatic force is produced to compress a DE in thickness and expand its area. A Maxwell stress (σ_v) originates from the electrostatic force which can be expressed by Eqn. (1).

$$\sigma_{\mathrm{V}} = \varepsilon'\varepsilon_0(\Phi/(H\,\lambda^{-2}))^2 = \varepsilon'\varepsilon_0\varphi^2 \qquad (1)$$

[1]Corresponding author, email: liang.jiang@mydit.ie

where ε' is the relative permittivity of the DE material, ε_0 is the permittivi ty of the free space (8.85×10^{-12} F/m), λ is the stretch ratio in the two mutually perpendicular planes normal to the thickness direction and H is the thickness which decreases to h ($h = H\lambda^{-2}$) when a voltage is applied and φ is the electric field which equals the applied high voltage (HV) Φ divided by the thickness of the DE. Electromechanical instability (EMI), which is also termed pull-in instability, is highlighted as the most significant failure mode for DEs when they are used as electromechanical actuators [6, 7]. This kind of failure occurs when the thickness of a DE falls below a certain threshold and the equivalent Maxwell pressure exceeds the compressive stress of the elastomer film. Its positive feedback leads to an unstable compression of the elastomer material which reduces thickness further and consequently breakdown ensues [8].

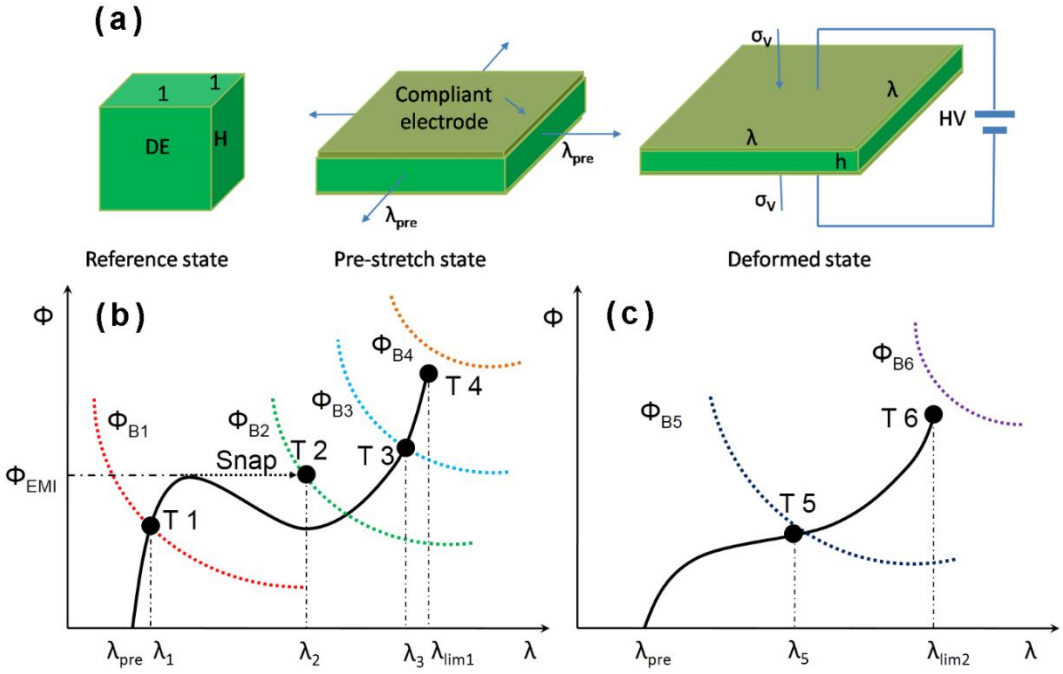

Fig. 1. Electromechanical Instability versus Stretch Ratio. (a) A membrane of a dielectric elastomer subject to a voltage reduces in thickness and expands in area; (b) and (c) six failure points T1-T6, depending on where the two curves $\Phi(\lambda)$ and $\Phi_B(\lambda)$ are positioned.

As can be seen from Fig. 1(a) a DE membrane deforms in response to applied forces and voltages. In the reference state, subject to no force and no voltage, the square sample is of unit area and thickness H. Because each crosslinked polymer chain in a DE has a large number of monomers, the crosslinks have negligible effect on the polarization of the monomers, that is to say the elastomer polarizes freely similar to a polymer melt. This similarity was used in the theory proposed by Zhao and Suo [9-11]. Therefore, the effect of the voltage on the deformation of the elastomer is equivalent to an equi-biaxial Maxwell stress. In the absence of an externally applied mechanical load, the equation of state is $\sigma_v = \sigma(\lambda)$. In the equi-biaxial pre-stretched state, subject to mutually perpendicular forces P, the sample is stretched to length λ_{pre} and the force gives rise to a mechanical stress $\sigma_{pre} = PH/\lambda_{pre}$. The mechanical stress and the Maxwell stress together cause the elastomer to deform, so that [9]:

$$\sigma_{pre} + \sigma_v = \sigma(\lambda) \quad (2)$$

Combined with Eqn. (1), the equation for $\Phi(\lambda)$ can be expressed as

$$\Phi(\lambda) = H\lambda^{-2}\sqrt{\left(\sigma(\lambda) - \sigma_{pre}\right)/\varepsilon'\varepsilon_0} \quad (3)$$

Consequently, the voltage-stretch curve is not monotonic and the electric breakdown voltage Φ_B equals $\varphi_B H/\lambda^2$ [12]. For an ideal DE, the dielectric constant and breakdown field φ_B is independent of the stretch λ [10]. Based on these considerations, six failure modes of DEs can occur and are depicted in Figs. 1(b) and (c) in terms of EMI, electrical breakdown and tensile strength limit. As shown in Fig. 1 (b), the first mode (T1) indicates a DE achieving a small voltage-induced strain and being punctured at λ_1 due to electrical breakdown voltage Φ_{B1} prior to the onset of EMI. Other researchers have described the portion of the voltage-stretch curve beyond T1, where a DE is capable of large voltage-induced deformation, as a region of snap-through instability [12]. They and others [13] recognised that an elastomer may survive EMI without electrical breakdown and stabilise with a much reduced thickness. In this region, the voltage again increases and attains point T2 where the DE fails when the voltage reaches the electromechanical instability voltage Φ_{EMI}. If failure does not occur at T2 the DE continues to exhibit more pronounced EMI and the film thins excessively, finally resulting in electrical breakdown at the point (λ_2, Φ_{B2}). Points T3 and T4 indicate where DEs survive EMI, but the failure at T3 is a result of electrical breakdown voltage Φ_{B3} at a stretch ratio of λ_3. The failure at T4 is as a result of reaching the tensile strength limit of the material at λ_{lim1} without experiencing electrical breakdown. Fig. 1 (c) depicts two modes of DE failure when EMI is eliminated. At point T5 the DE fails due to electrical breakdown voltage Φ_{B5} at a stretch ratio of λ_5. At point T6 a DE fails at the limit of tensile strength (λ_{lim2}).

Therefore, as described in the previous paragraph, the voltage-induced strain of DEs can be enhanced by suppressing EMI. Zhao [14] investigated EMI using a polyacrylate DE film (VHB 4910, 3M) and found that EMI can be eliminated if the soft DEs stiffen sufficiently under deformations. Thus, many kinds of novel DEs with stiffening properties were fabricated by means of an interpenetrating network [15], swelling with a solvent [16] and pre-stretch [10, 12, 17-19]. Pre-stretch is a convenient and effective method of removing EMI from soft DEs mainly because of the strain stiffening effect. Outstanding research into the elimination of EMI for VHB 4910 using pre-stretch has been carried out based on the Neo-Hookean [20-22], Arruda-Boyce [9], Mooney-Rivlin [23, 24], Yeoh [25, 26], Ogden [27] and Gent models [11-13, 19, 28, 29]. However, most of these investigations were conducted without fitting experimental data obtained from equi-biaxial tensile testing. Moreover, of the models using strain invariants, the Neo-Hookean, Yeoh and Gent models do not employ the second strain invariant I_2, so cannot capture the predominant stiffening effect [30] at higher strains. As with other material models, for the Ogden model, errors can occur when it is applied outside the deformation range from which its parameters were calculated [31]. Therefore, it is essential to find an appropriate model to characterise the mechanical behaviour of DEs and investigating the influence of pre-stretch on EMIs using other DE materials is essential. In this work, a modified Gent model incorporating the second strain invariant I_2 was employed to study the EMI of VHB 4910. SR/BT based DEs, which have the capability of overcoming the drawbacks of VHB 4910 such as high viscoelasticity [32, 33], low thermal stability and high sensitivity to environmental degradation [34], were also fabricated. Moreover, the influence of filler content onto the elimination of EMI was investigated.

2. Experimental

2.1 Materials

VHB 4910 is a polyacrylate purchased from the 3M Company in the UK. A commercial polymer, dimethylsiloxane (LSR4305 DEV, Bluestar Ltd., U.S.A), consisting of two parts (part A and part B) was used for fabricating the silicone DE samples; NYOGEL 756G (Nye Lubricants, Inc., USA) was the conductive carbon grease used for the compliant electrodes. Both $BaTiO_3$ and dopamine hydrochloride (melt point 248-250°C) were purchased from Sigma-Aldrich Co. LLC. The average particle size of the BT was approximately 1μm and the particle density was 6.08 g/ml at 25°C.

2.2 DP-BT and DE film preparation

A detailed description of film preparation was provided in a previous paper [35], so only a brief description of sample preparation appears here. Initially 10 g of BT was dispersed in 50 ml of ethanol-water mixture having a mass ratio of 1:1 and stirred for 30 minutes in order to graft an OH^- functional group onto the particle surfaces. The solution was then added to 450 ml of deionized water with 1g of dopamine hydrochloride also added to the suspension. Thereafter, the suspension was stirred at 60°C overnight before being subjected to ultrasonic shaking for 30 min. The DP-BT particles were subsequently removed and washed using deionized water and finally dried at 60°C in a vacuum to avoid oxidization of the dopamine.

Two methods were used to prepare the DE films for bubble inflation and electromechanical testing. For bubble inflation and deflation, a two-part polymer was first mixed at a ratio of 1:1 before BT with the required filler content was added to the silicone matrix. The DE composites containing BT were mechanically stirred to give consistent high levels of dispersibility. The mixtures were then degassed in a vacuum to remove trapped air bubbles and then poured into moulds. The samples were degassed for 1.5 hours and solidified in an oven at a temperature of 80 °C for approximately 12 hours. This allowed DE samples of 0.3 mm and 2 mm thickness to be fabricated using two alternative moulds. For electromechanical tests, the two parts of the SR polymer were mixed at a weight ratio of 1:1 and dissolved in heptane. Then, BT or DP-BT particles were added to the solution to provide samples containing the required percentage particle weights of 10%, 20% and 40%. In order to achieve uniform dispersion of the SR and fillers in heptane, the solution was subjected to ultrasonic shaking for 20 minutes. Finally, the mixture was poured into a watch glass and heated for 8 hours at 80°C in a water bath in an airing chamber.

2.3 Characterization

The dielectric properties of VHB 4910, SR/BT and SR/DP-BT films were determined using a broadband dielectric spectrometer (Novocontrol, Germany) at room temperature in the frequency range of 0.1 Hz to 10 MHz. The DE films were placed on cells which were disposable gold-plated flat electrodes with diameters of 20 mm and thickness of 2 mm.

The relation between equibiaxial stress and stretch ratio was studied using a bubble inflation test system [36]. As shown in Fig. 2, it induces dynamic equi-biaxial mechanical stresses in elastomer samples by hydraulically inflating and deflating them using silicone oil. Disc samples of 2 mm thickness and 50 mm nominal diameter were prepared for physical testing. The samples were held in the bubble inflation system's inflation orifice. In initial static tests, pressure was applied to the

samples causing them to inflate. During inflation (or deflation) the system's vision system uses two CMOS (complementary metal-oxide semiconductor) cameras to record the movement of the centres of specific points aligned at the pole on the surface of each sample. Stress values were simultaneously derived from the applied pressure and bubble geometry, with strain (or stretch ratio) values calculated from the change in circumferential distance between the centres of the points on the bubble surface using three dimensional position coordinates obtained from the vision system output. Hence, the relation between stress and strain (or stretch ratio) is obtained simultaneously. In this work, the equi-biaxial stress-stretch curves for SR based DEs, which were thereafter used in Eqn. (3), were obtained over a wide equi-biaxial stretch range from 1 to 5 using the bubble inflation test system.

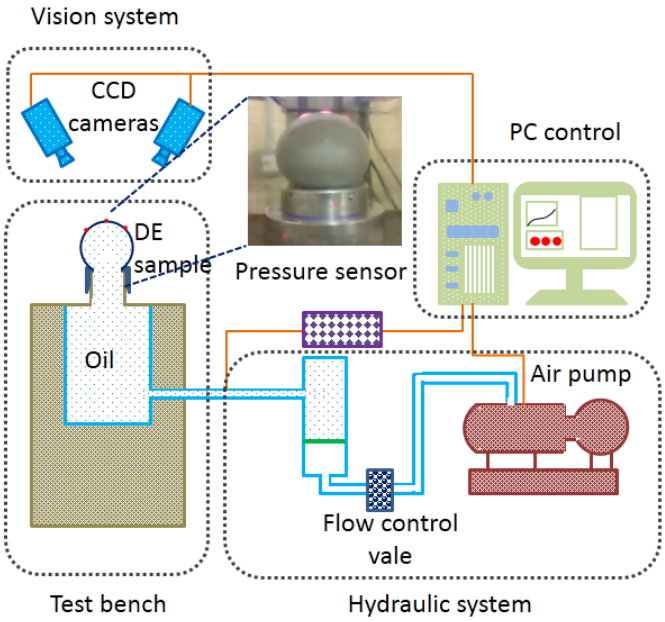

Fig. 2. The bubble inflation test system and a sample under test.

The relation between applied voltage and actuated stretch ratio was obtained in an in-house electromechanical test system consisting of a camera, a biaxial clamp to apply pre-stretching and a high DC voltage power supply (Fig. 3). Prior to use, these samples were coated with the compliant electrode. Then, samples were clamped with a range of pre-stretch ratios applied to them and the camera recorded changes in their area for incremental increases in electric field of 0.5 kV per 10 seconds at 10 seconds intervals. Finally, the initial area (A_0) and the actuated area (A) were accurately measured using AutoCAD software. The area strain s_a was calculated using the following expression.

$$s_a = (A - A_0)/A_0 \qquad (4)$$

Furthermore, the actuated stretch ratio was determined and is dependent on the voltage-induced strain expressed as

$$\lambda = \sqrt{1 + s_a} \qquad (5)$$

As the volume of a DE is assumed to be constant (Poisson's ratio $v \approx 0.5$) irrespective of whether a high voltage is applied or not, the area strain (s_a) has a simple relationship with the thickness strain (s_z) as given by Eqn. (6).

$$s_a = 1/\left(1-|s_z|\right)-1 \qquad (6)$$

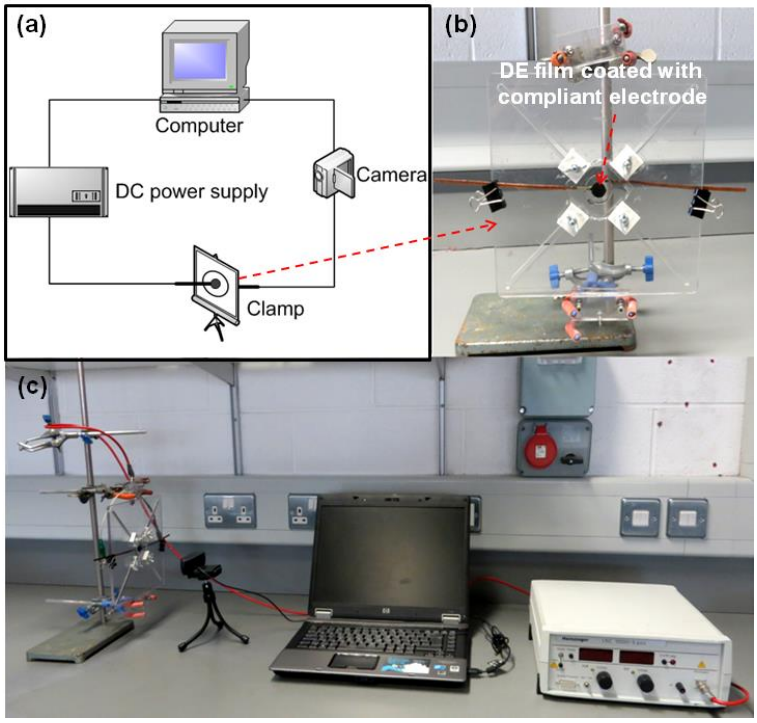

Fig. 3. The electromechanical test system in this research: (a) the working schematic of the test system; (b) the pre-stretch fame used for pre-stretching DE films; (c) the image of the system.

3. Results and discussions

3.1 The influence of pre-stretch on dielectric constant

Though pre-stretch has an influence on the dielectric constant of DE materials, it was considered that this minimal influence could be ignored [16]. It was shown that the dielectric constant of polyacrylate film decreased by a few percent when pre-stretched to $\lambda = 5$ [37]. Furthermore, it was found that the dielectric constant of SR was virtually unchanged during pre-stretch in the experiments described here [38]. Thus, the dielectric constants of VHB 4910 and the SR based DEs were regarded as independent of the deformation in this research. The dielectric constants obtained at 1 kHz for VHB 4910 and the pure SR were 4.7 and 3.0 respectively. The dielectric constants of SR/BT composites and SR/DP-BT composites were as shown in Table 1.

Table 1. The dielectric constants of SR/BT composites and SR/DP-BT composites.

Filler content, wt%	ε' of SR / $BaTiO_3$ at 1 kHz	ε' of SR / DP-BT at 1 kHz
0	3.0	3.0
10	3.4	4.7
20	3.6	5.3
40	5.0	7.0

3.2 Stress-stretch behaviour of VHB 4910 and SR based DEs

As determined from Eqn. (3), a DE's voltage is a function of true stress. Thus, the investigation of the stress-stretch behaviour for all DEs is essential in their development and application. Generally, stress-stretch curves can be acquired by tensile testing or deduced from a free energy function for the mechanical model under conditions of different load modes such as uniaxial, equi-biaxial and pure shear deformations. However, due to the constraints of the VHB 4910 sample size in the test, the stress-stretch curve was only determined for stretch ratios from 1 to approximately 2 (Fig. 4) in bubble inflation test system. Therefore, it was necessary to introduce a suitable mechanical model providing an improved understanding of stress-stretch behaviour at larger stretch ratios.

The strain energy function from a modified Gent model [39, 40] which includes a logarithmic term for I_2 is expressed as

$$\mathrm{W}(I_1, I_2) = -\frac{\mu J_m}{2}\ln\left(1-\frac{I_1-3}{J_m}\right)+c_2\ln\left(\frac{I_2}{3}\right) \qquad (7)$$

where μ is the shear modulus, C_2 is the material constant and J_m is the constant limiting value for I_1-3, accounting for finite chain extensibility. I_1 and I_2 are the first and second even powered strain invariants respectively. Under equi-biaxial loading

$$I_1 = 2\lambda^2 + \frac{1}{\lambda^4} \qquad (8)$$

$$I_2 = \lambda^4 + \frac{2}{\lambda^2} \qquad (9)$$

The true stress associated with stretch is given by

$$\sigma(\lambda) = \lambda\frac{\partial W(\lambda)}{\partial\lambda} \qquad (10)$$

Substituting Eqns. (7), (8) and (9) into Eqn. (10) gives:

$$\sigma(\lambda) = \frac{2\mu J_m\left(\lambda^2 - 1/\lambda^4\right)}{J_m - 2\lambda^2 - 1/\lambda^4 + 3} + \frac{4C_2(\lambda^4 - 1/\lambda^2)}{\lambda^4 + 2/\lambda^2} \qquad (11)$$

For VHB 4910, J_m is approximately 120 [11, 25]. The experimental data was fitted to Eqn. (11) with μ = 0.01262 MPa, C_2 = 0.02711 and correlation co-efficiency was determined as (R^2) = 0.99448. Fig. 3 shows the stress-strain plots of VHB 4910 and SR and the curve fitting for VHB 4910. As can be seen from the figure, the true stress of VHB 4910 was larger than that of the pure SR sample below a stretch ratio of around 2.5. However, the situation was reversed above this stretch ratio. The true stress was about 3 MPa for both VHB 4910 and SR at a stretch ratio of 5.

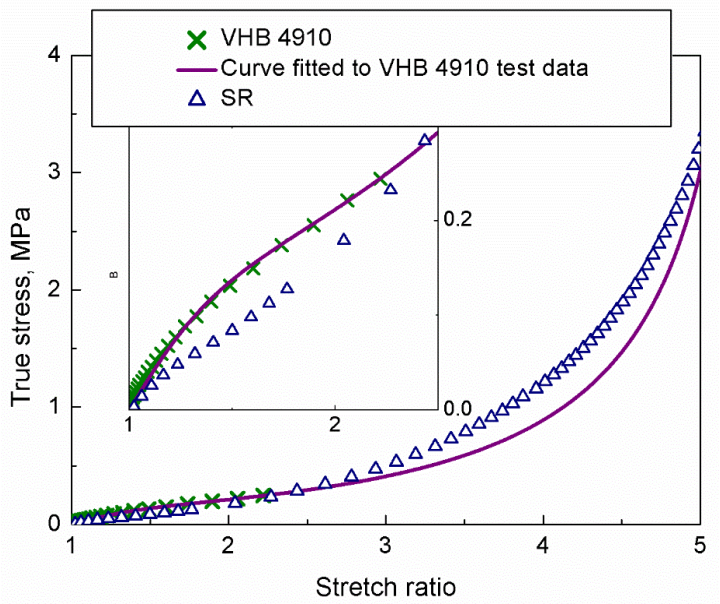

Fig. 4. Plots of true stress of VHB 4910 and SR against stretch ratio.

The stress-stretch curves of SR composites with different BT and DP-BT content are presented in Fig. 5. All samples used in these tests exhibited hyperelastic deformation. For the particle content range tested, it appeared that the 40 wt% of particle compounds were the weakest and the 10 wt% the strongest. This is probably due to the presence of agglomerates, which have been observed in previous work [35], acting as stress raisers and also leading to a decrease of filler-matrix interactions [41]. As shown, for stretch ratios up to 5, the true stresses of SR/DP-BT samples were in the approximate stress range of 3 MPa to 6 MPa when subjected to equi-biaxial loading. However, the stresses for the SR/BT composites were in the approximate range of 1.5 MPa to 8 MPa for the same stretch ratios and for the same particle contents. True stress increased approximately linearly up to stretch ratios of about 1.2. The rate of increase in stress tended to be less for increases in stretch for higher filler concentrations, unsurprisingly indicating that stiffness reduced as filler content increased. Moreover the increased quantity of amino groups in the composite significantly reduced the degree of crosslinking in silicone rubber by reacting with the curing agent [42, 43].

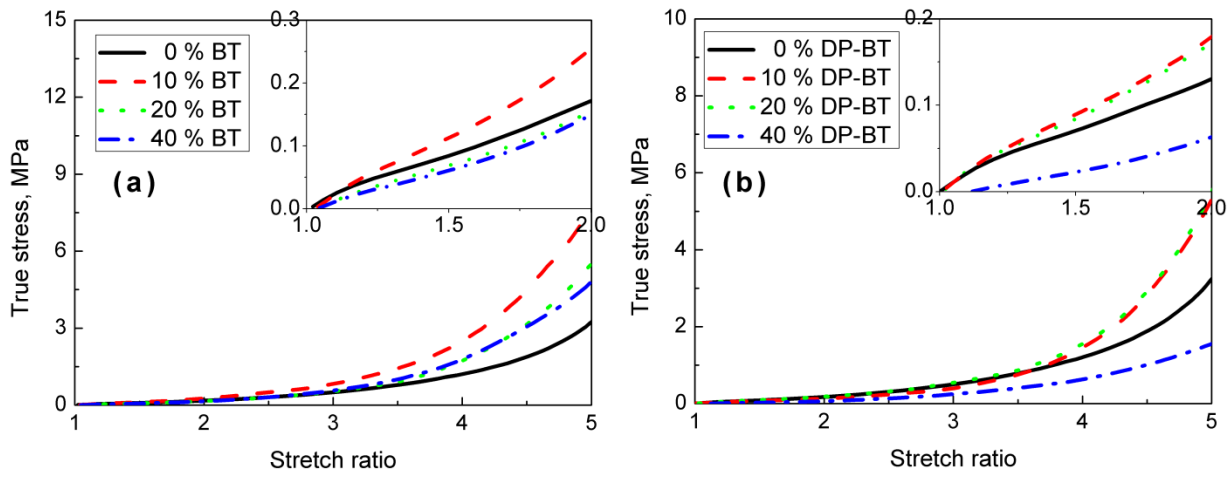

Fig. 5. Curves of true stress versus stretch ratio for SR composites with varying (a) BT content and (b) DP-BT content. (The inserts show the low stretch ratio behaviour for each composite).

3.3 EMI of VHB 4910 and SR based DEs

The voltage Φ dependent on stretch ratio for DEs can be obtained in accordance with Eqn. (3). For given values of λ_{pre} and Φ, the DE was in one of a number of equilibrium states. Fig. 6 depicts a range of curves for voltage versus stretch ratio for (a) VHB 4910 and (b) SR. The curves were obtained by varying the pre-stretch ratio (λ_{pre}) in the range 1 to 3. σ_{pre} was determined for all values of pre-stretch from the $\sigma(\lambda)$ curves shown in the figure. As can be seen from Fig. 6 (a) and (b), when the λ_{pre} is small (1 to 1.6) for VHB 4910 and SR, the voltage-stretch curve exhibited a maximum value of Φ before declining to values of approximately 10 kV and 4 kV respectively. It is possible for EMI to appear on the DE surfaces at and beyond these maximum values without failure occurring. Initially, for small voltages, the deformation of the DE increased with increasing voltage. Thereafter, when the voltage exceeded the value for Φ_{EMI}, the DE film drastically deformed with a pronounced increase in area strain and concurrent thinning of the test sample. Ultimately, the applied electric field reached a level where breakdown ensued resulting in the failure of the DE. When λ_{pre} was large (above 2), the voltage-stretch curve increased monotonically without EMI occurring, so the DEs only suffered failure at electrical breakdown. Furthermore, it can be seen from Figs. 6 (a) and (b) that the critical voltage Φ_{EMI} decreased as a result of increasing the pre-stretch. For VHB 4910, Φ_{EMI} declined from about 28 kV to 10 kV between λ_{pre} = 1.0 and λ_{pre} = 1.6, while for pure SR, Φ_{EMI} decreased from 7 kV to 4 kV for the same pre-stretch range.

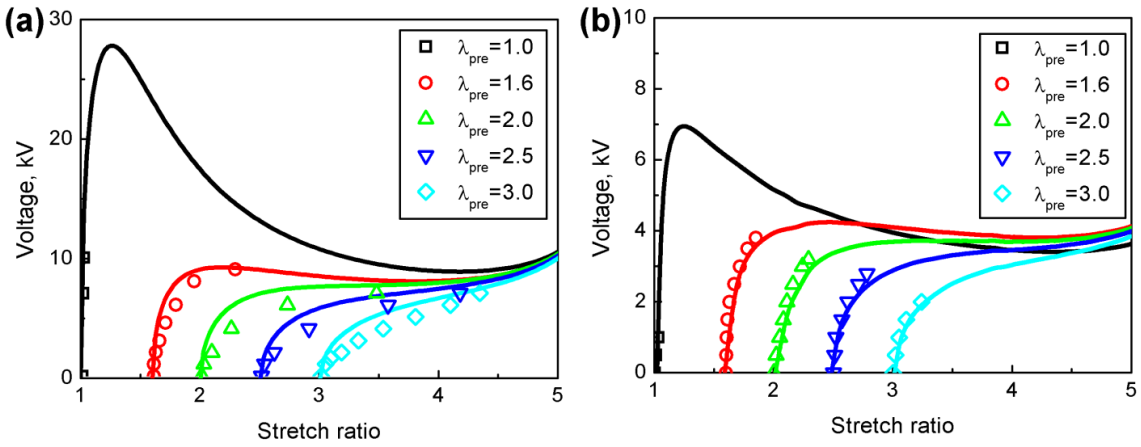

Fig. 6. Actuation of (a) VHB 4910 and (b) SR under equi-biaxial loading. The plots were created from experimental data obtained using the electromechanical test system and the curves depicted in color were derived from Eqn. (3).

Fig. 7 shows the different sample configurations when a voltage was applied across a VHB 4910 film. As can be observed from Fig. 7 (a), the DE surface coated with carbon electrode is uniform without the occurrence of EMI, whereas at a high voltage the surface creases and wrinkles indicating the presence of EMI on the DE (Fig. 7 (b)).

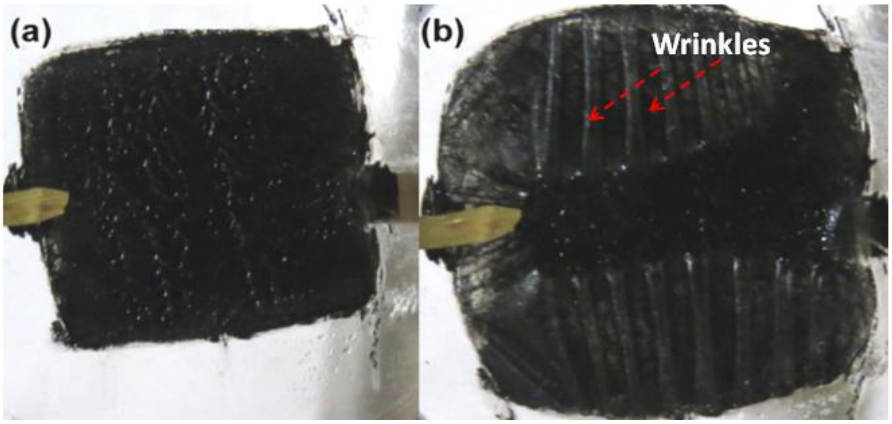

Fig. 7. The morphology of VHB 4190 films (a) the uniform area without instability; (b) the creased area with instability exhibiting EMI.

As the stiffness of a DE material can be tuned by pre-stretch, the secant modulus dependent on the stretch ratio was studied in this work. Fig. 8 shows the secant modulus and actuated area strain of VHB 4910 and SR samples varying with pre-stretch ratio. As can be seen from the figure, all curves of secant moduli related with per-stretch ratios are parabolic indicating that the stiffness of DEs decreased at the beginning and then increased till tensile failure. This means the EMI is readily suppressed by applying a pre-stretch ratio from which the secant moduli rose. Thus, the possibility of suppressing EMI for VHB 4910 was only achievable when applying a pre-stretch ratio above 2.0 (the secant moudulus is a minimum at the ratio of about 2.0), while it is necessary to apply a stretch ratio above 1.6 for SR. It is well known that the magnitude of elastic modulus is related to intermolecular force. As shown in the figure, both VHB 4910 and SR are capable of achieving

large voltage-induced deformations for low values of elastic moduli where the intermolecular forces are at a minimum, indicating a freer elongation of the molecular chains when subjected to a high voltage. It has been reported that the VHB 4910 film achieved a large voltage-induced strain of up to 158% by employing an equi-biaxial pre-stretch ratio of 3 [44]. In this research, for VHB 4910, a maximum voltage-induced strain of 200% was achieved at a pre-stretch ratio of 2.0 by applying a large electric field. Beyond this level of pre-stretch, the voltage-induced strain unexpectedly decreased, possibly due to the greater pre-strain inducing a higher modulus as a result of strain stiffening. For SR, the curve of the secant modulus and actuated area strain are parabolic. This is in line with the behaviour of VHB 4910. The maximum voltage-induced strain was also achieved at a pre-stretch of 2.0, but with a lower modulus. By comparison with VHB 4910, SR achieved a smaller voltage-induced strain probably due to the lower dielectric constant.

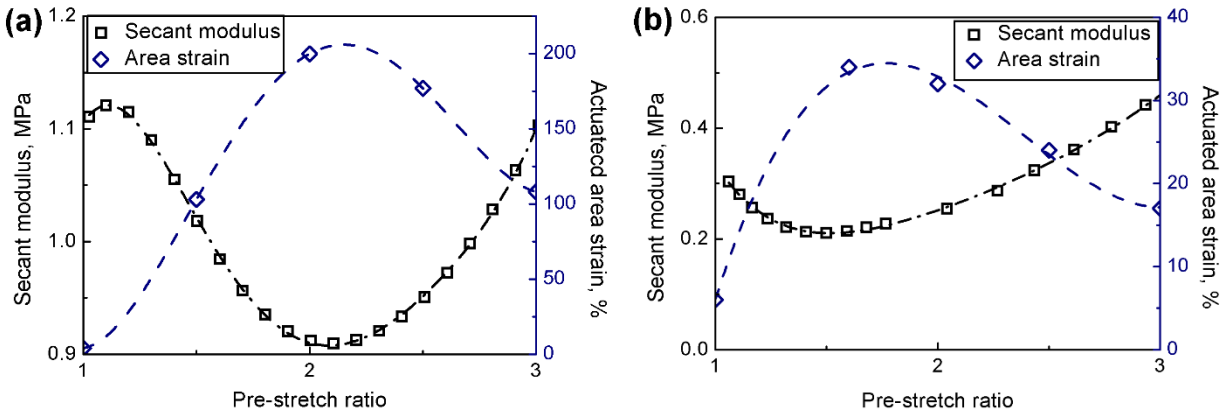

Fig. 8. The secant modulus and actuated area strain of (a) VHB 4910 and (b) SR plotted against pre-stretch ratio.

Fig. 9 shows the voltage-stretch curves with varied pre-stretch ratios for SR/BT composites and SR/DP-BT composites respectively. As can be observed from these curves, it was found that the region of 'snap through' was reduced by adding fillers or increasing the pre-stretch ratio. Additionally, the electromechanical voltage decreased as filler content increased for both SR/BT composites and SR/DP-BT composites. Furthermore, N-shaped voltage-stretch curves for all composites were transformed to monotonically increasing curves by applying a pre-stretch ratio of 2.5 or more, indicating the suppression of EMI. Moreover, it was also found that EMI was alleviated by the addition of BT or DP-BT. For the SR/BT composites, though EMI persisted without pre-stretch, it was initially eliminated by applying a small pre-stretch ratio of 1.6 to the SR based DE with 20 wt% BT, and then disappeared with a pre-stretch ratio of 2.0 for all the films tested. For the SR/DP-BT composites, EMI was clearly removed at a pre-stretch ratio of 1.6 for the composites of SR/10 wt% DP-BT and SR/20 wt% DP-BT. This was not so for the SR/40 wt% DP-BT composite which still exhibited EMI. When comparing SR/BT composites with SR/DP-BT composites, the SR based DEs filled with DP-BT were observed to be less likely to exhibit EMI at small pre-stretch ratios. The trends observed in these curves of voltage against stretch ratio for SR based DEs were similar to the finding using acrylate VHB 4910 in Lu's work [11].

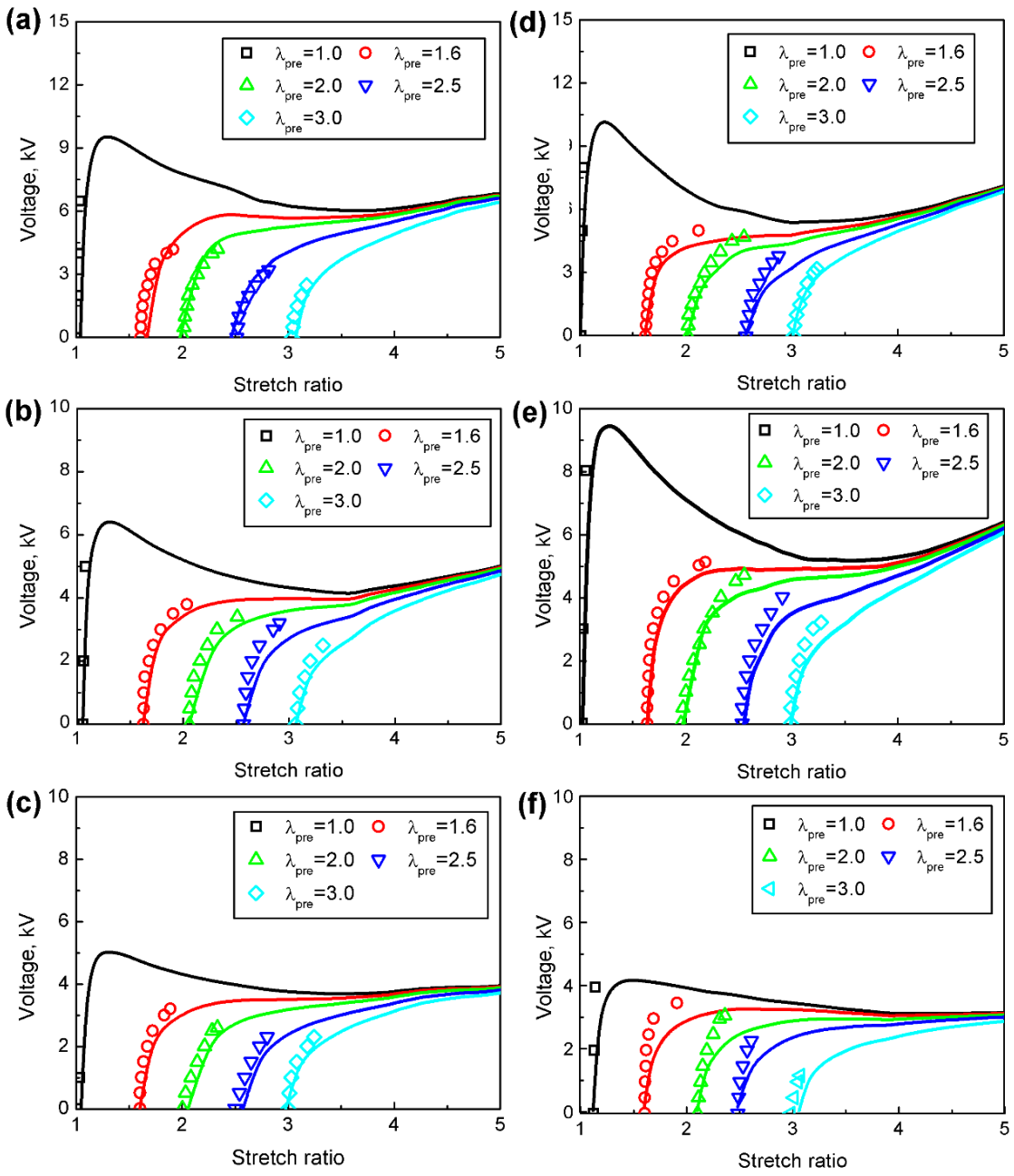

Fig. 9. The voltage-stretch curves with various pre-stretch ratios for SR composites with (a) 10 wt%, (b) 20 wt% and (c) 40 wt% BT and SR composites with (d) 10 wt%, (e) 20 wt% and (f) 40 wt% DP-BT respectively. (The plots were created using stress-stretch curves in accordance with Eqn. (3) and the individual points shown on the graphs were obtained from experimentation)

It is inappropriate to compare the onset voltage at which point EMI occurs for DEs with different thickness. Thus, in this work the electric field (φ_{EMI}) at which EMI began to occur was employed. Table 2 shows the values of the electric field φ_{EMI} during the application of a range of pre-stretch ratios for all the DEs tested. As can be seen from this table, the φ_{EMI} of VHB 4910 hardly changed although the pre-stretch increased from 1.0 to 1.6. However, the φ_{EMI} of SR based DEs increased significantly with increases in pre-stretch ratio. It also can be seen that with the addition of fillers, the φ_{EMI} of all the DE composites without pre-stretching decreased except for the two composites of SR/10 wt% BT and SR/40 wt% BT.

Table 2. The values of the electric field (φ_{EMI}) at which EMI commenced occurring under the condition of different pre-stretch ratios for all DEs in this experiment.

Polymer (specific type)	***H(mm)***	φ_{EMI}, **V/μm**				
		(λ_{pre} = 1.0)	**(λ_{pre} = 1.6)**	**(λ_{pre} = 2.0)**	**(λ_{pre} = 2.5)**	**(λ_{pre} = 3.0)**
VHB 4910	1.00	44	44	NEI	NEI	NEI
Pure SR	0.30	36	88	151	NEI	NEI
SR/10 wt% BT	0.34	40	92	NEI	NEI	NEI
SR/20 wt% BT	0.34	31	109	NEI	NEI	NEI
SR/40 wt% BT	0.22	40	NEI	NEI	NEI	NEI
SR/10 wt% DP-BT	0.50	31	NEI	NEI	NEI	NEI
SR/20 wt% DP-BT	0.46	33	NEI	NEI	NEI	NEI
SR/40 wt% DP-BT	0.50	22	53	81	NEI	NEI

* NEI = No Electromechanical Instability

Fig. 10 shows that the secant modulus and actuated area strain are dependent on pre-stretch ratio for both the SR/BT and SR/DP-BT composites. As can be observed from the figure, all curves are parabolic. As stated previously, EMI can be suppressed by modifying the stiffening properties. Thus, as shown in the figure, all SR based DE have the possibility of eliminating EMI by applying a pre-stretch ratio of about 1.6 because the secant modulus increased from its lowest value, indicating of the onset of the strain stiffening effect. The root and crest in all tests was located within the same range of stretch ratios from 1 to 3. Furthermore, the maximum actuated area strain was achieved for all SR based DEs for a pre-stretch ratio of approximately 1.6. For the SR/BT composites, the maximum voltage-induced strain varied with increasing filler content. The minimum strain of 0.34 was achieved by the SR composite with 10 wt% BT with a secant modulus of 0.3 MPa at a stretch ratio of 1.6. Meanwhile, the maximum strain of 58%, the largest amongst those of SR/BT composites, was achieved by the composite of SR/20 wt% BT with a secant modulus of around 0.19 MPa at a stretch ratio of 1.6. Thereafter, the maximum strain (56%) decreased slightly with increasing filler content at 40 wt% at a secant modulus of 0.17 MPa for a stretch ratio of 1.6. For the SR/DP-BT composites, the actuated area strain was a maximum of 78% for a filler content of 20 wt%. Though, of all the DE films, the composite of SR/40 wt% DP-BT had the lowest secant modulus, the largest voltage-induced strain for this composite was surprisingly 40% at a pre-stretch ratio of 2.0. This outcome could primarily be due to defects introduced into the composite by the decrease in electric field at failure.

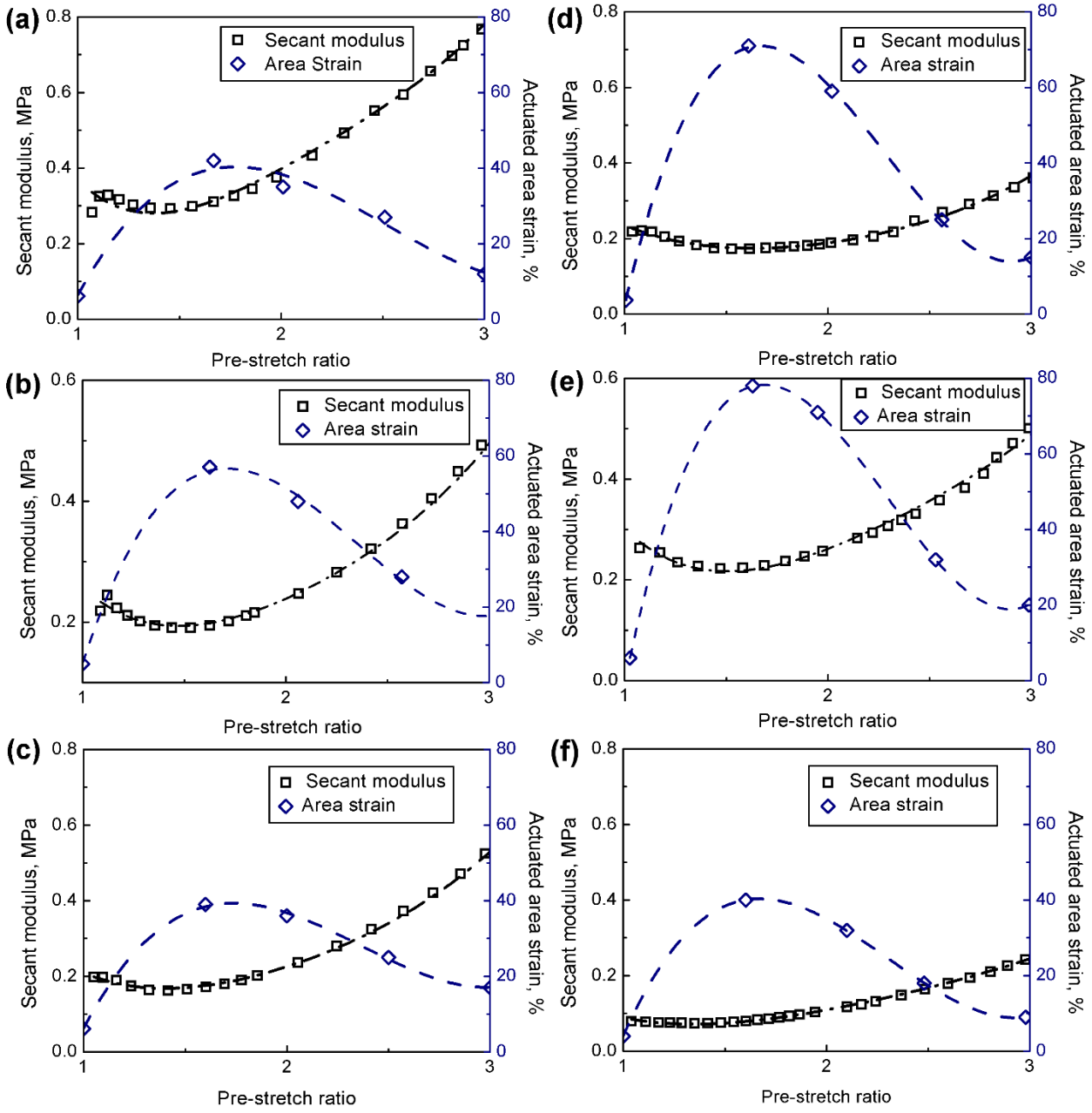

Fig. 10. The secant modulus and actuated area strain versus pre-stretch ratio for SR composites with (a) 10 wt%, (b) 20 wt% and (c) 40 wt% BT, and SR composites with (d) 10 wt%, (e) 20 wt% and (f) 40 wt% DP-BT respectively.

4. Conclusion

When high voltages were applied, the strain stiffening effect was observed in samples that had pre-stretch ratios of approximately 1.6 for SR based DEs and 2.0 for the VHB 4910 film. This strain stiffening provided the opportunity of suppressing EMI which is evidenced by the absence of EMI in the bulk of the tests carried out on DEs with different particle contents. SR based DEs achieved large voltage-induced strains of up to 78% in the experiments. Both the polyacrylate VHB 4910 and SR inevitably suffered from EMI in tests where no equi-biaxial pre-stretch was applied prior to testing or when low equi-biaxial pre-stretch ratios were applied prior to testing. However, the instability was assuaged by means of the addition of fillers in the SR based DEs. For the composite of SR/10 wt% DP-BT, EMI was clearly eliminated at a pre-stretch ratio of 1.6 and above, while instability disappeared at a pre-stretch ratio of above 2.0 for the polyacrylate films. Universally, pre-stretch had a significant influence on the voltage-induced strain of all DE films. For all the membranes, the maximum voltage-induced strain was achieved when the composites were pre-stretched to ratios in the range 1.6 to 2.0. Furthermore, with the addition of fillers, strain was increased for the SR composites in all tests. Among all the composites, the maximum voltage-induced strain of 78% was obtained for the SR/20 wt% DP-BT composite at a pre-stretch ratio of 1.6. SR/20 wt% DP-BT is a potential alternative to VHB 4910 in terms of its capacity to alleviate EMI and offer large voltage-induced deformation.

Acknowledgements

The authors gratefully acknowledges the support provided by the DIT Fiosraigh Dean of Graduate Students Award.

References

[1] K. Ig Mo, J. Kwangmok, K. Ja-Choon, J.-D. Nam, L. Young Kwan, C. Hyouk-Ryeol, Development of Soft-Actuator-Based Wearable Tactile Display, Robotics, in IEEE Transactions on Robotics, 24 (2008) 549-558.
[2] T. Sugimoto, A. Ando, K. Ono, Y. Morita, K. Hosoda, D. Ishii, K. Nakamura, A lightweight push-pull acoustic transducer composed of a pair of dielectric elastomer films, The Journal of the Acoustical Society of America, 134 (2013) EL432-EL437.
[3] M. Giousouf, G. Kovacs, Dielectric elastomer actuators used for pneumatic valve technology, Smart Materials and Structures, 22 (2013) 6.
[4] T.G. McKay, T.A. Gisby, I.A. Anderson, Artificial muscles harvesting sensational power using self-sensing, Proc. SPIE 6056, Electroactive Polymer Actuators and Devices (EAPAD) 2014, 905603.
[5] C. Jean-Mistral, T. Vu-Cong, A. Sylvestre, On the power management and electret hybridization of dielectric elastomer generators, Smart Materials and Structures, 22 (2013) 12.
[6] X. Zhao, Z. Suo, Electromechanical instability in semicrystalline polymers, Applied Physics Letters, 95 (2009) 031904.
[7] X. Zhao, Z. Suo, Electrostriction in elastic dielectrics undergoing large deformation, Journal of Applied Physics, 104 (2008) 123530.
[8] J.-S. Plante, S. Dubowsky, Large-scale failure modes of dielectric elastomer actuators, International Journal of Solids and Structures, 43 (2006) 7727-7751.

[9] S.J.A. Koh, T. Li, J. Zhou, X. Zhao, W. Hong, J. Zhu, Z. Suo, Mechanisms of large actuation strain in dielectric elastomers, Journal of Polymer Science Part B: Polymer Physics, 49 (2011) 504-515.
[10] X.H. Zhao, Z.G. Suo, Theory of Dielectric Elastomers Capable of Giant Deformation of Actuation, Physical Review Letters, 104 (2010) 4.
[11] T. Lu, J. Huang, C. Jordi, G. Kovacs, R. Huang, D.R. Clarke, Z. Suo, Dielectric elastomer actuators under equal-biaxial forces, uniaxial forces, and uniaxial constraint of stiff fibers, Soft Matter, 8 (2012) 6167-6173.
[12] B. Li, H. Chen, J. Zhou, Z. Zhu, Y. Wang, Polarization-modified instability and actuation transition of deformable dielectric, EPL (Europhysics Letters), 95 (2011) 37006.
[13] B. Li, H. Chen, J. Qiang, S. Hu, Z. Zhu, Y. Wang, Effect of mechanical pre-stretch on the stabilization of dielectric elastomer actuation, Journal of Physics D: Applied Physics, 44 (2011) 155301.
[14] X. Zhao, Q. Wang, Harnessing large deformation and instabilities of soft dielectrics: Theory, experiment, and application, Applied Physics Reviews, 1 (2014) 021304.
[15] Z. Suo, J. Zhu, Dielectric elastomers of interpenetrating networks, Applied Physics Letters, 95 (2009) 232909.
[16] Z. Suo, Theory of dielectric elastomers, Acta Mechanica Solida Sinica, 23 (2010) 549-578.
[17] T. Lu, C. Keplinger, N. Arnold, S. Bauer, Z. Suo, Charge localization instability in a highly deformable dielectric elastomer, Applied Physics Letters, 104 (2014) 022905.
[18] D. De Tommasi, G. Puglisi, G. Zurlo, Inhomogeneous deformations and pull-in instability in electroactive polymeric films, International Journal of Non-Linear Mechanics, 57 (2013) 123-129.
[19] C. Keplinger, T. Li, R. Baumgartner, Z. Suo, S. Bauer, Harnessing snap-through instability in soft dielectrics to achieve giant voltage-triggered deformation, Soft Matter, 8 (2012) 285-288.
[20] L. Zhang, Q. Wang, X. Zhao, Mechanical constraints enhance electrical energy densities of soft dielectrics, Applied Physics Letters, 99 (2011) 171906.
[21] H. Yong, X. He, Y. Zhou, Dynamics of a thick-walled dielectric elastomer spherical shell, International Journal of Engineering Science, 49 (2011) 792-800.
[22] T. He, X. Zhao, Z. Suo, Dielectric elastomer membranes undergoing inhomogeneous deformation, Journal of Applied Physics, 106 (2009) 083522.
[23] Y. Liu, L. Liu, K. Yu, S. Sun, J. Leng, An investigation on electromechanical stability of dielectric elastomers undergoing large deformation, Smart Materials and Structures, 18 (2009) 095040.
[24] Y. Liu, L. Liu, S. Sun, Z. Zhang, J. Leng, Stability analysis of dielectric elastomer film actuator, Science in China Series E: Technological Sciences, 52 (2009) 2715-2723.
[25] A. Schmidt, P. Rothemund, E. Mazza, Multiaxial deformation and failure of acrylic elastomer membranes, Sensors and Actuators A: Physical, 174 (2012) 133-138.
[26] B.-X. Xu, R. Mueller, M. Klassen, D. Gross, On electromechanical stability analysis of dielectric elastomer actuators, Applied Physics Letters, 97 (2010) 162908.
[27] L. Yanju, L. Liwu, Z. Zhen, L. Jinsong, Dielectric elastomer film actuators: characterization, experiment and analysis, Smart Materials and Structures, 18 (2009) 095024.
[28] T. Li, S. Qu, W. Yang, Electromechanical and dynamic analyses of tunable dielectric elastomer resonator, International Journal of Solids and Structures, 49 (2012) 3754-3761.
[29] B. Li, L. Liu, Z. Suo, Extension limit, polarization saturation, and snap-through instability of dielectric elastomers, International Journal of Smart and Nano Materials, 2 (2011) 59-67.

[30] C.O. Horgan, M.G. Smayda, The importance of the second strain invariant in the constitutive modeling of elastomers and soft biomaterials, Mechanics of Materials, 51 (2012) 43-52.
[31] G. Marckmann, E. Verron, Comparison of Hyperelastic Models for Rubber-Like Materials, Rubber Chemistry and Technology, 79 (2006) 835-858.
[32] J.J. Sheng, H.L. Chen, L. Liu, J.S. Zhang, Y.Q. Wang, S.H. Jia, Dynamic electromechanical performance of viscoelastic dielectric elastomers, Journal of Applied Physics, 114 (2013) 8.
[33] S. Rosset, B.M. O'Brien, T. Gisby, D. Xu, H.R. Shea, I.A. Anderson, Self-sensing dielectric elastomer actuators in closed-loop operation, Smart Materials Structures, 22 (2013) 104018.
[34] R. Shankar, T.K. Ghosh, R.J. Spontak, Dielectric elastomers as next-generation polymeric actuators, Soft Matter, 3 (2007) 1116-1129.
[35] L. Jiang, A. Betts, D. Kennedy, S. Jerrams, Improving the electromechanical performance of dielectric elastomers using silicone rubber and dopamine coated barium titanate, Materials & Design, 85 (2015) 733-742.
[36] Y. Zhou, S. Jerrams, A. Betts, G. Farrell, L. Chen, The influence of particle content on the equi-biaxial fatigue behaviour of magnetorheological elastomers, Materials & Design, 67 (2015) 398-404.
[37] G. Kofod, P. Sommer-Larsen, R. Kornbluh, R. Pelrine, Actuation response of polyacrylate dielectric elastomers, Journal of intelligent material systems and structures, 14 (2003) 787-793.
[38] A. Trols, A. Kogler, R. Baumgartner, R. Kaltseis, C. Keplinger, R. Schwodiauer, I. Graz, S. Bauer, Stretch dependence of the electrical breakdown strength and dielectric constant of dielectric elastomers, Smart Materials and Structures, 22 (2013) 5.
[39] R.W. Ogden, G. Saccomandi, I. Sgura, Fitting hyperelastic models to experimental data, Computational Mechanics, 34 (2004) 484-502.
[40] E. Pucci, G. Saccomandi, A Note on the Gent Model for Rubber-Like Materials, Rubber Chemistry and Technology, 75 (2002) 839-852.
[41] D. Yang, M. Tian, D. Li, W. Wang, F. Ge, L. Zhang, Enhanced dielectric properties and actuated strain of elastomer composites with dopamine-induced surface functionalization, Journal of Materials Chemistry A, 1 (2013) 12276-12284.
[42] S.E. Shim, A.I. Isayev, Ultrasonic Devulcanization of Precipitated Silica-Filled Silicone Rubber, Rubber Chemistry and Technology, 74 (2001) 303-316.
[43] B. Adhikari, D. De, S. Maiti, Reclamation and recycling of waste rubber, Progress in Polymer Science, 25 (2000) 909-948.
[44] R. Pelrine, R. Kornbluh, Q. Pei, J. Joseph, High-Speed Electrically Actuated Elastomers with Strain Greater Than 100%, Science, 287 (2000) 836-839.